ENSO's Spatial Patterns and Their Impact on Atlantic Tropical Cyclone Activity

2012-12-13

Abstract

Near equatorial Pacific warming anomalies (ENSO) have a well documented influence on seasonal Atlantic tropical cyclone (TC) activity. A large body of work has focused on capturing such activity using empirical warming indices with the goal of forecasting a variety of long-range events – including seasonal Atlantic TC counts a subject of societal and scientific interest. Unfortunately, such indices have had limited predictive capabilities. Here we show that to fully capture the role ENSO plays with regard to Atlantic TC activity, it is necessary to monitor both the intensity and location of anomalous Pacific warming. We examined the shifting patters of Pacific ocean warming and found that the most anomalous warming is shifting westward. Based on this observation, we proposed a new spatial ENSO index (S-ENSO) that provides improved forecasting abilities compared to standard warming-based indices, especially when it comes to overcoming the ENSO spring predictability barrier. [I need a final 2-3 sentence to position these findings within a broader context]

1 Introduction

Seasonal tropical cyclone (TC) forecasting has become an active field of research [5, 4, 3, 13]. While such forecasts do not predict frequency or intensity of landfalling hurricanes, aggregate TC statistics such as counts are regarded as valuable by the reinsurance industry and are useful for forecasting the environment's response to seasonal TC activity – for example ocean heat transport or phytoplankton blooms. A primary driver of seasonal TC activity are the large-scale conditions over the Atlantic basin and any reasonable attempt at skillful seasonal prediction should be able to reproduce these conditions [9], even if synoptic-scale (*i.e.* African Easterly Waves, *etc.*) and stochastic events cannot be accounted for [14, 6].

One of the well-documented influencers of Atlantic TC activity on seasonal timescales through large-scale conditions is the El-Niño Southern Oscillation (ENSO): the quasi-periodic cycle of warming and cooling of the near equatorial Pacific sea surface temperatures (SST). Some of the earliest empirical studies proposed that enhanced convection as a result of anomalous Eastern Pacific Ocean warming is associated with strong westerly upper tropospheric wind over the Caribbean basin and tropical Atlantic, resulting in low TC activity during ENSO's warm phase (El Niño) and high TC activity during its cold phase (La Niña) [10]. Other studies have suggested that ENSO influences Atlantic TC activity via tropospheric warming [18].

For the past 50 years, numerous attempts to represent such a cycle using empirical warming-based indices have been made. Indices such as NINO1+2 and NINO3.4 are constructed by averaging the sea surface temperature (SST) anomalies of static oceanic regions and are subsequently related to Atlantic TC activity [19]. However, a closer examination of the number of TCs on a seasonal-scale as a function of ENSO's phase shows that the difference of TC counts between each phase is not statistically significant (see Figure 1).

To improve on traditional NINO indices, some research proposed to monitor several regions concurrently [20, 16] or focus on the Central Pacific [1]. Warming in the Central Pacific, known as El Niño Modoki (or Central Pacific ENSO), where warm waters are surrounded by cold ones has been observed with increased frequency since the 1990s. Such changes have been attributed to anthropogenic global warming [23] as well as natural climate variability [22] and might affect Atlantic TC landfalling probabilities [12].

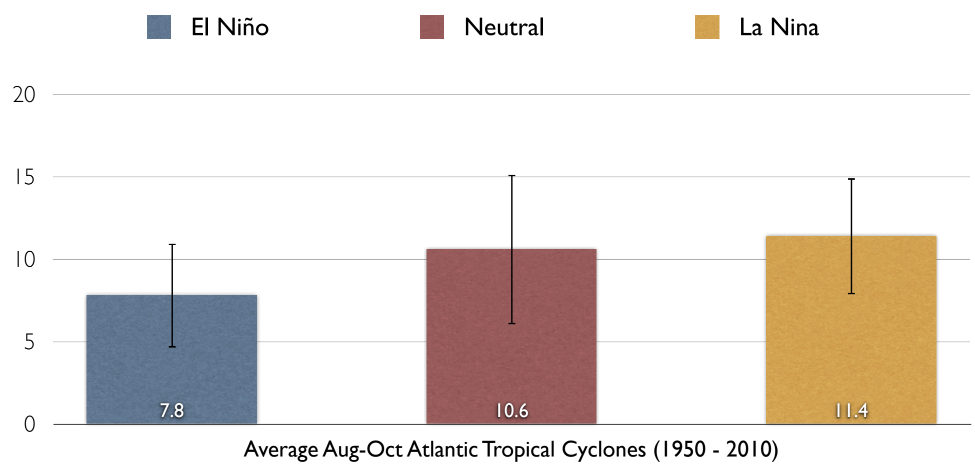

Figure 1: The mean August-October Atlantic TC counts for Niño (16 years), Neutral (39 years) and Niña (10 years). The ENSO phases are based on NINO3.4 from 1950-2010. Error bars denote one standard deviation. This figure shows that while there are notable differences in TC counts based on the phase of ENSO, the large variability of TC counts make discerning ENSO's impact uncertain. The NINO3.4 index was built using ERSSTV3. TC counts are from the Unisys best track archive. See methods for full details.

Given that ENSO affects the large-scale conditions over the Atlantic through anomalous warming and its associated wind shear, it is not only important to monitor the intensity of warming along the equatorial Pacific – something traditional NINO indices do – but also to capture the location of the warming. We propose a distance-based ENSO index (S-ENSO for spatial ENSO) that tracks the longitude of highest SST anomaly in the tropical Pacific. We demonstrate its robustness in predicting seasonal Atlantic TC activity as well as resolving the large-scale conditions over the Atlantic. Such an index, coupled with other seasonal prediction methods based on Atlantic variables may prove to be a significant addition to dynamical and statistical TC forecast models.

2 Shifting of ENSO

Given the increasing number of studies reporting a shift in ENSO's warming patterns [1, 11, 23, 15, 12], we examine empirically the extent of such a shift. For every month from January 1979 to December 2010, we monitor the longitude of the warmest 10° latitude by 40° longitude region in the Pacific (see methods for details). As it can be seen in Figure 2 there has been a distinct westward shift in the longitude of the warmest Pacific region. This may explain how traditional NINO indices were initially successful in capturing the impact Pacific warming might have on Atlantic TCs, but as the warming gradually shifted westward they have grown less accurate.

Figure 2: The annual mean longitude of the warmest SST anomaly region in the Pacific ($1979-2010$). The figure shows a clear westward shift of the warmest region in the Pacific. $R^2 = 0.54$ $p < 0.01$

	TCs	Major Hurricanes	NTC	PDI	ACE
S-ENSO	**-0.75**	**-0.59**	**-0.74**	**-0.68**	**-0.73**
Nino1+2	-0.51	-0.46	-0.46	-0.4	-0.42
Nino 3	-0.51	-0.51	-0.48	-0.44	-0.45
Nino 4	-0.32	-0.47	-0.32	-0.3	-0.31
Nino 3.4	-0.47	-0.53	-0.46	-0.43	-0.45

Table 1: Linear correlation coefficients between the June-October S-ENSO and August-October Atlantic TC activity. The highest score for each category is highlighted in **bold**. All S-ENSO correlations are significant at 95% level

3 An S-ENSO index for shifting warming patters

We propose that the spatial distribution of Pacific Ocean warming might provide better predictive insights into the ENSO-Atlantic TC activity relationship than warming anomalies alone. We introduce the S-ENSO index that tracks the longitude of the warmest SST anomaly region between 6° S - 36° N and 90° W - 140° E. Monitoring the spatial distribution of warming has several advantages over traditional intensity-based indices that monitor a fixed region: First, it inherently accounts for any changes in ENSO's warming patters. Second, it is intimately related to the deep convection and associated distribution of the Walker circulation as a result of anomalous warming. Finally, unlike warming-based indices, it is robust to any temporal trends in the data.

The index is built by first averaging monthly SST anomalies over a certain month range and subsequently recording the location of the highest warming anomaly. Here we present the performance of the June-October S-ENSO index (see methods). We restrict our attention to satellite-era only data and this analysis spans data from 1979 until 2010. Table 1 shows S-ENSO's linear correlation coefficients with various quantities that summerize August-October Atlantic TC activity: number of tropical cyclones, number of major hurricanes, power dissipation index (PDI) [7], accumulated cyclone energy (ACE) [2], and net tropical cyclone energy (NTC) [8]. The significant improvement over traditional static NINO indices, especially with regards to cumulative statistics such as ACE and NTC, indicates that S-ENSO resolves the large-scale conditions over the Atlantic as well as the in-season TC precursors more accurately than static warming-base indices.

In addition to providing better in-season accuracy than traditional NINO indices, S-ENSO is more robust to the ENSO spring predictability barrier [21]. Given that all ENSO indices, including S-ENSO, can be calculated for any month range we investigated each index' robustness to increasing lead times based on all possible month ranges up to a certain month (referred to here as lead month). Figure 5 shows the performance of S-ENSO as a function of months from which SST anomalies are averaged before building the index. When S-ENSO is built using Northern Hemisphere winter SSTs, its performance declines significantly. The performance gradually improves through the spring and summer months.

Figure 3 shows the performance of each NINO index as well as S-ENSO as a function of lead time. S-ENSO is significantly more robust than traditional NINO indices to the Spring predictability barrier. Give the 30 degrees of freedom in the data (N=32; df = N-2), the traditional NINO indices do not provide significant correlations (above 0.345) with Aug-Oct TCs until July, as opposed to March for S-ENSO. Furthermore, the improved accuracy remains significant from January until October. Therefore, if dynamical models can resolve the Pacific spatial warming patterns as represented by S-ENSO, then dynamical models could potentially have significant skill in predicting

August-October TC activity.

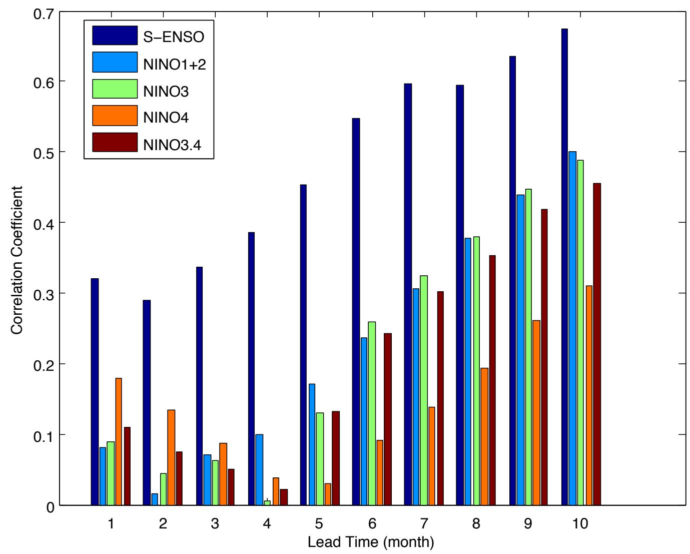

Figure 3: The linear correlation coefficients between different ENSO indices and Atlantic August-October TC counts. The x-axis denotes the last month used to build each index (see methods). The indices increase in accuracy as we move closer to the TC season, however S-ENSO performance is not as severely affected by the ENSO predictability barrier as traditional NINO indices.

	NINO (N = 16)	Neutral (N= 36)	NINA (N = 10)
Mean Aug-Oct TC counts	7.8	11.06	11.44
Standard deviation	3.17	4.37	3.54

Table 2: The mean Aug-Oct TC counts based on the phase of ENSO. NINO years we defined as years with more than $+1°$C warming anomaly. NINA years were years with less than $-1°$C anomaly. Neutral years were years with warming between $-1°$C and $+1°$C. Given the large overlap between each group we cannot reject the null hypothesis that any two quantities are equal.

4 Summary of Methods

4.1 TC Counts as a Function of ENSO's phase

ENSO phase data was acquired from the NOAA Climate Prediction Center. NINO and NINO episodes were based on a threshold of +/- 1°C for the Oceanic Niño Index (ONI) [3 month running mean of ERSST.v3b SST anomalies in the Niño 3.4 region (5°N-5°S, 120°-170°W)], based on centered 30-year base periods updated every 5 years. Cold and warm episodes are defined when the threshold is met for a minimum of 5 consecutive over-lapping seasons.

4.2 S-ENSO

The S-ENSO index is computed by first averaging the SST anomalies over the June-October period to accurately capture ENSO's evolution prior to and during the Atlantic hurricane season (August-October). We then search the tropical Pacific (5°S-30°N) for a region of similar size to traditional ENSO indices that has the highest mean SST anomaly over the June-October period. We repeat this procedure for each year from 1979 to 2010. Monthly SST anomalies we computed from the ERSSTV3 monthly SST dataset [17]. See Figure 4.

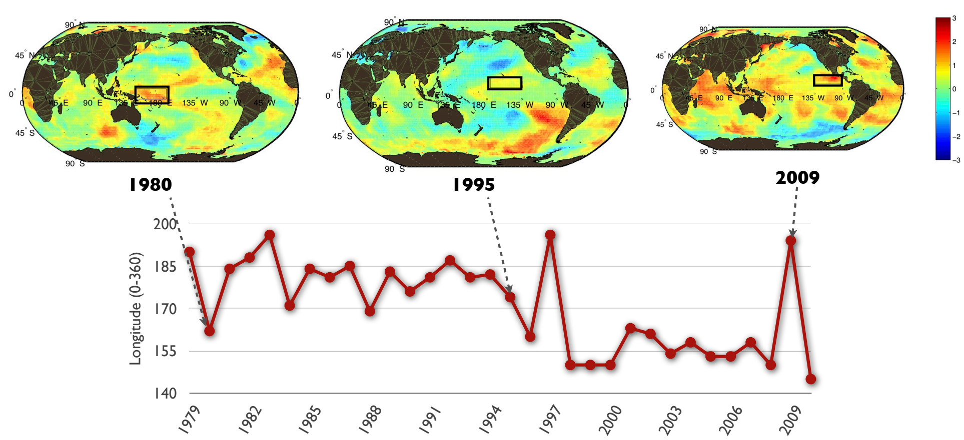

Figure 4: A schematic demonstrating how the S-ENSO index is built. First, SST anomalies over a certain month range are computed resulting in maps similar to those above. Next, we search the tropical Pacific for the region with the highest mean SST warming anomaly. Finally, we record the longitude of that region. We repeat this procedure for all years from 1979-2010.

4.3 Lead Times Analysis

For the lead time analysis we tested the robustness of each index, by computing all possible indices as a function of the start and end months of the SST anomalies used to calculate the index. See Figure 5.

We built similar tables as in Figure 5 for all the NINO indices. To test the relative robustness of each index to the ENSO spring predictability barrier, we average the performance of each index up to a given month (lead month). To do so, we average all the rows under each end month column. For example, S-ENSO had a mean correlation with Aug-Oct TCs of 0.61 for a July lead. This was obtained by averaging all the rows under July end month in Figure 5. The mean correlation of 0.61 means that if we knew all SST anomalies up to July we could on average explain 36% of Aug-Oct variance.

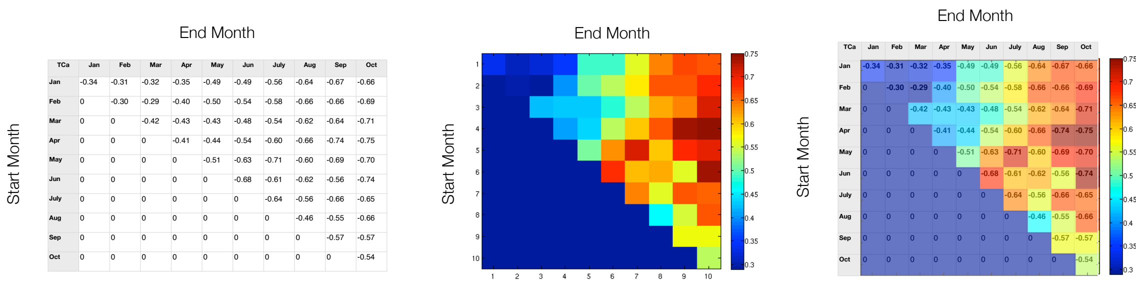

TCa	Jan	Feb	Mar	Apr	May	Jun	July	Aug	Sep	Oct
Jan	-0.34	-0.31	-0.32	-0.35	-0.49	-0.49	-0.56	-0.64	-0.67	-0.66
Feb	0	-0.30	-0.29	-0.40	-0.50	-0.54	-0.58	-0.66	-0.66	-0.69
Mar	0	0	-0.42	-0.43	-0.43	-0.48	-0.54	-0.62	-0.64	-0.71
Apr	0	0	0	-0.41	-0.44	-0.54	-0.60	-0.66	-0.74	-0.75
May	0	0	0	0	-0.51	-0.63	-0.71	-0.60	-0.69	-0.70
Jun	0	0	0	0	0	-0.68	-0.61	-0.62	-0.56	-0.74
July	0	0	0	0	0	0	-0.64	-0.56	-0.66	-0.65
Aug	0	0	0	0	0	0	0	-0.46	-0.55	-0.66
Sep	0	0	0	0	0	0	0	0	-0.57	-0.57
Oct	0	0	0	0	0	0	0	0	0	-0.54

Figure 5: The linear correlation coefficient of every possible S-ENSO index obtained by first averaging SST month anomalies between Start Month (rows) and End Month (columns). S-ENSO's performance increases as the index includes SST anomalies during the Atlantic TC season (June-October).

References

[1] K. Ashok, S.K. Behera, S.a. Rao, H. Weng, and T. Yamagata. El Niño Modoki and Its Possible Teleconnection. *J. Geophys. Res*, 112(10.1029), 2007.

[2] G D Bell, M S Halpert, R C Schnell, R W Higgins, J Lawrimore, V E Kousky, R Tinker, W Thiaw, M Chelliah, and a Artusa. Climate Assessment for 1999. *Bulletin of the American Meteorological Society*, 81(6):S1–S50, 2000.

[3] James B. Elsner, Thomas H. Jagger, Michael Dickinson, and Dail Rowe. Improving Multiseason Forecasts of North Atlantic Hurricane Activity. *Journal of Climate*, 21(6):1209–1219, 2008.

[4] Jb Elsner, X. Niu, and Aa Tsonis. Multi-Year Prediction Model of North Atlantic Hurricane Activity. *Meteorology and Atmospheric Physics*, 68(1):43–51, 1998.

[5] J.B. Elsner and Cp Schmertmann. Improving Extended-Range Seasonal Predictions of Intense Atlantic Hurricane Activity. *Weather and Forecasting*, 8(3):345–351, 1993.

[6] K. Emanuel, R. Sundararajan, and J. Williams. Hurricanes and GLobal WArming. *Bull. Am. Meteorol. Soc*, 89:347–367, 2008.

[7] Kerry Emanuel. Increasing Destructiveness of Tropical Cyclones over the Past 30 Years. *Nature*, 436(7051):686–688, 2005.

[8] S.B. Goldenberg, C.W. Landsea, a.M. Mestas-NuÑEz, and W.M. Gray. the Recent Increase in Atlantic Hurricane Activity: Causes and Implications. *Science*, 293(5529):474, 2001.

[9] W. M. Gray. Global View of the Origin of Tropical Disturbances and Storms. *Monthly Weather Review*, 96(10):669700, 1968.

[10] W.M. Gray. Atlantic Seasonal Hurricane Frequency. Part I: El NiÑO and 30 Mb Quasi-Biennial Oscillation Influences. *Mon. Wea. Rev*, 112(9):1649–1668, 1984.

[11] H.Y. Kao and J.Y. Yu. Contrasting Eastern-Pacific and Central-Pacific Types of ENSO. *Journal of Climate*, 22(3):615–632, 2009.

[12] Hye-Mi Kim, Peter J. Webster, and Judith a. Curry. Impact of Shifting Patterns of Pacific Ocean Warming on North Atlantic Tropical Cyclones. *Science*, 325(5936):77–80, 2009.

[13] P.J. Klotzbach and W.M. Gray. Twenty-Five Years of Atlantic Basin Seasonal Hurricane Forecasts. *Geophysical Research Letters*, 36:L09711, 2009.

[14] T.R. Knutson, J.J. Sirutis, S.T. Garner, I.M. Held, and R.E. Tuleya. Simulation of the Recent Multidecadal Increase of Atlantic Hurricane Activity Using an 18-Km-Grid Regional Model. *Bulletin of the American Meteorological Society*, 88(10):1549–1565, 2007.

[15] J.S. Kug, F.F. Jin, and S.I. an. Two Types of El Niño Events: Cold Tongue El Niño and Warm Pool El Niño. *Journal of Climate*, 22(6):1499–1515, 2009.

[16] H.L. Ren and F.F. Jin. Niño Indices for Two Types of ENSO. *Geophysical Research Letters*, 38(4):L04704, 2011.

[17] R.W. Reynolds, N.a. Rayner, T.M. Smith, D.C. Stokes, and W. Wang. an Improved in Situ and Satellite Sst Analysis for Climate. *Journal of Climate*, 15(13):1609–1625, 2002.

[18] Bh Tang and Jd Neelin. ENSO Influence on Atlantic Hurricanes Via Tropospheric Warming. *Geophys. Res. Lett*, 31:L24204, 2004.

[19] K.E. Trenberth. the Definition of El Niño. *Bulletin of the American Meteorological Society*, 78(12):2771–2777, 1997.

[20] K.E. Trenberth and D.P. Stepaniak. Indices of El Niño Evolution. *Journal of Climate*, 14(8):1697–1701, 2001.

[21] P.J. Webster and S. Yang. Monsoon and ENSO: Selectively Interactive Systems. *Quarterly Journal of the Royal Meteorological Society*, 118(507):877–926, 1992.

[22] a.T. Wittenberg. Are Historical Records Sufficient to Constrain ENSO Simulations. *Geophys. Res. Lett*, 36:L12702, 2009.

[23] S.W. Yeh, J.S. Kug, B. Dewitte, M.H. Kwon, B.P. Kirtman, and F.F. Jin. El Niño in a Changing Climate. *Nature*, 461(7263):511–514, 2009.